Simulation of the f–d transitions of lanthanide ions in YPO_4 using quantum-chemical calculations*

Hu Liu-Sen(胡流森), Wen Jun(闻 军)†, Yin Min(尹 民), and Xia Shang-Da(夏上达)

Department of Physics, University of Science and Technology of China, Hefei 230026, China

(Received 23 August 2011; revised manuscript received 9 September 2011)

We constructed an effective one-electron Hamiltonian by using the 4f/5d energies and eigenvectors obtained from the first-principles calculation with the relativistic self-consistent discrete variational Slater software package (DV-Xα). From the effective Hamiltonian, we obtained the crystal-field and spin-orbit interaction parameters for the 4f and 5d electrons of lanthanide ions (Ce^{3+}, Pr^{3+}, Nd^{3+} and Eu^{3+}) doped in YPO_4, and these parameters were used to calculate the $4f^N$–$4f^{N-1}5d$ transition. Comparison with experiments shows that the obtained parameters are reasonable and the excitation spectra can be well predicted.

Keywords: crystal field, spectroscopic, YPO_4, *ab initio*

PACS: 78.20.Bh, 78.40.–q, 71.10.–w, 71.20.Eh **DOI:** 10.1088/1674-1056/21/1/017801

1. Introduction

Lanthanide ions have been widely used in luminescent materials for display, lasers and scintillators.[1,2] The parametric crystal-field model for determining the energy levels within the $4f^N$ configuration of lanthanide ions in condensed matter environments was originally developed in the 1960s, and has been extended to the $4f^{N-1}5d$ configuration in recent years.[3–5] Although the parametric model has made great progress in determining the experimental energy levels and analysing optical spectra,[6,7] the application to the $4f^{N-1}5d$ configuration was usually limited because there are too many parameters to be fitted in the model. In addition, for interconfiguration transitions, the spectra consist mainly of broad vibronic bands, making the fitting more difficult.[8]

One of the approaches to studying the electronic structure of the $4f^N$ and $4f^{N-1}5d$ configurations of lanthanides is the first-principles calculation,[9–11] which has been useful for examining the spectra of Ce^{3+} in solids. However, it is difficult to apply to the multi-electron configurations across the lanthanide series due to the one-electron approximation in most of the first-principles calculations. Seijo and coworkers[9] performed Hartree–Fock calculations combined with configuration interaction. This approach can be very accurate, but requires a large number of Slater determinants, which limits their calculation to Ce^{3+} and Yb^{2+} in hosts with high symmetry.

In this paper, we first apply the discrete variational slater software package (DV-Xα) method to obtain the one-electron 4f and 5d energies and their corresponding molecular orbitals by solving the one-electron Dirac equation, and then derive the crystal-field and spin-orbit interaction parameters with the model space method.[11,12] These parameters are then combined with the parameters for the quasi free-ion multi-electron Hamiltonian for the $4f^N$ and $4f^{N-1}5d$ configurations[13,14] to calculate the energy levels and wave functions for the $4f^N$ and $4f^{N-1}5d$ configurations. With the obtained energy levels and wave functions, the transition intensities, and hence the absorption spectra, are calculated in a straightforward way.

2. Models and calculations

2.1. The parametric Hamiltonian model

The parametric Hamiltonian model has had great success in energy levels calculations and spectrum analysis. The energy levels, i.e. E_i, of the $4f^N$ con-

*Project supported by the National Natural Science Foundation of China (Grant Nos. 10874173, 10904139, 11074315, 11074245, 11047147, and 11011120083).

†Corresponding author. E-mail: wenjunkd@mail.ustc.edu.cn

© 2012 Chinese Physical Society and IOP Publishing Ltd

figuration of lanthanide ions in a crystal can be analysed with a parametric model employing an effective-operator Hamiltonian, i.e. H, expressed as a matrix that is diagonalized to give the corresponding wave functions $\psi_{\rm i}$

$$(H - E_{\rm i})\psi_{\rm i} = 0, \tag{1}$$

where

$$H = H_{\rm AT} + H_{\rm CF} + H_{\rm ADD.} \tag{2}$$

Here, $H_{\rm AT}$ comprises the pseudo-free ion or atomic Hamiltonian, including all interactions that are spherically symmetric; $H_{\rm CF}$ is the operator comprising the non-spherically symmetric crystal field; and $H_{\rm ADD}$ contains other interactions, which is a perturbation compared with $H_{\rm AT}$ and $H_{\rm CF}$.

$$\begin{aligned} H_{\rm AT} =\ & E_{\rm AV} + \sum_k F^k {\rm f}_k + \sum_i \zeta_f s_i \cdot l_i + \alpha L(L+1) \\ & + \beta G(G_2) + \gamma G(R_7) + \sum_s T^s t_s \\ & + \sum_k P^k p_k + \sum_j M^j m_j, \end{aligned} \tag{3}$$

$$H_{\rm CF} = \sum_{k,q,i} B_q^k C_q^k(i). \tag{4}$$

For $4{\rm f}^{N-1}5{\rm d}$, the interactions between the $4{\rm f}^{N-1}$ core and 5d electron, which are defined as $H_{\rm fd}$, should be added in the atomic Hamiltonian

$$\begin{aligned} H_{\rm fd} =\ & \Delta_E({\rm fd}) + \sum_k F^k({\rm fd}){\rm f}_k({\rm fd}) + \sum_k G^k({\rm fd}){\rm g}_k({\rm fd}) \\ & + \zeta_d A_{\rm SO}({\rm dd}). \end{aligned} \tag{5}$$

The additional crystal-field on the 5d electron should also be added to the crystal-field Hamiltonian

$$H_{\rm CF}({\rm dd}) = \sum_{k,q} B_q^k({\rm dd}) C_q^k({\rm dd}). \tag{6}$$

The meanings of the various operators and parameters in Eqs. (3)–(6) have been defined in Ref. [14].

2.2. The DV-Xα calculation and the model-space effective Hamiltonian method

The DV-Xα program was originally developed for quantum chemical calculations of the electronic structure properties of molecular systems by Ellis and coworkers,[15] and was further developed by Adachi and co-workers.[16] The program employs the discrete variational method for a cluster that is isolated or embedded in microcrystal, in which α is the exchange-correlation potential parameter and is fixed at 0.7 in this work. For effective calculation, by replacing the integral calculations with a summation of the calculated results at sampling points – which has been found to be appropriate for the charge distribution – the DV-Xα method was performed not only for directly calculating the electronic states of lanthanides, but also on a preparatory basis to obtain the molecular orbitals for the further calculation of a many-electron system. In this work, we use a relativistic version, which therefore automatically includes the spin-orbit interaction.

The chosen cluster was composed of Ln^{3+} and its eight nearest neighbours, O^{2-}. To speed up the calculation, some of the inner orbitals were frozen, except 4f, 5s, 5p, 5d and 6s for Ln^{3+}, and 2s and 2p for O^{2-}. The molecular orbitals, which contain not only the centre-ion atomic orbitals – such as 4f and 5d of Ln^{3+} here, but also the atomic orbitals for ligands – were obtained by solving the one-electron DV-Xα Hamiltonian.

In order to construct an effective Hamiltonian $H_{\rm eff}$, only the eigenvalues and model-space projections of the eigenvectors dominated by the 4f or 5d components of the central trivalent lanthanide ion are needed. The model space that was then constructed was a small space spanned by 14 4f (or 10 5d) orbitals. From the $H_{\rm eff}$ constructed in the model space, the crystal-field parameters and spin-orbit parameters of the 4f electron (or 5d electron) were extracted in a straightforward way. Refer to Ref. [11] for further details.

2.3. Energy-level calculations and the absorption spectra of Ln^{3+}

The crystal field and spin-orbit interaction parameters were obtained from the calculations performed in this work. The additional parameters, such as the Coulomb interaction, the two-particle configuration interaction and the three-particle configuration interaction for $4{\rm f}^N$ electrons in Eq. (3), were taken directly from Ref. [13]. The parameters for the interactions between the f and d electrons, such as the direct and exchange Coulomb interactions, were derived

from the calculated free-ion values[14] with appropriate scaling.[8] The constructed Hamiltonian was then diagonalized to produce the eigenvalues and eigenvectors needed for the calculation of f–d transition intensities.

The calculation of the electric dipole matrix elements of $-erC_q^1$ (C_q^1 is the spherical tensor operator) for the transitions between the states of the $4f^N$ and $4f^{N-1}5d$ configuration is straightforward and not described here. There is a displacement of the equilibrium positions of the ligands in the 5d states relative to the 4f states, as the 5d orbitals are more spread out and interact more strongly with ligands than the 4f orbitals. The experimental spectra showed that most intensities were in the vibronic bands. Here, we simulate the vibronic bands by assuming that the superposition of several vibration modes gives rise to a vibronic band of Gaussian shape. The energy difference between the original zero-phonon line and the maximum of the Gaussian vibronic band corresponds to half of the Stokes shift between the absorption and emission maxima. Furthermore, we adopt the standard approximation that the intensities of the vibronic bands are proportional to the square of the electric dipole moment operator evaluated between the initial and final electronic states.

3. Results and discussion

The space group of YPO_4 is $I4_1/amd$ (the space group number is 141). The doped Ce^{3+} ions substitute for the Y^{3+} ions occupying the sites of D_{2d} symmetry. The nonzero 4f crystal-field parameters are B_0^2, B_0^4, B_4^4, B_0^6 and B_4^6, and the parameters for 5d are B_0^2, B_0^4 and B_4^4. The calculated parameters for Ce^{3+}, Pr^{3+}, Nd^{3+} and Eu^{3+} in YPO_4, and the fitting parameters, are listed in Table 1. The crystal-field parameters are real as the D_{2d} symmetry group contains a rotation operation about the Y-axis by π. It shows clearly that the calculated crystal-field parameters decrease slowly across the lanthanide series due to the increase in the nuclear charges, as expected. The strength of the crystal-field parameters is reduced as the electron orbitals are pulled closer to the nucleus. This effect is greater than that of the contraction of the crystal lattice by the decrease in the ionic radius of the lanthanide ion (reduction of the central ion-ligand distance). The calculated B_0^2(d) is larger than the value derived from the measured energy levels. This is easy to understand: B_0^2(d) is related to the long-range interaction compared with B_0^4(d) and B_4^4(d) when we choose a small cluster which only contains the eight nearest neighbours, O^{2-}, and the central lanthanide ions.

Table 1. Comparison of the crystal-field and spin-orbit parameter values for Ce^{3+}, Pr^{3+}, Nd^{3+} and Eu^{3+} in YPO_4, and the values for Ce^{3+} in LuPO4 derived from the measured energies (units: cm^{-1}).

	Parameters	$Ce^{3+a)}$	$Pr^{3+a)}$	$Nd^{3+a)}$	$Eu^{3+a)}$	$Ce^{3+b)}$
4f	B_0^2(ff)	27	26	24	22	26
	B_0^4(ff)	242	215	189	146	263
	B_4^4(ff)	–1073	–1006	–933	–765	–1247
	B_0^6(ff)	–1384	–1072	–848	–628	–1270
	B_4^6(ff)	227	205	189	171	148
	ζ_{4f}	770	903	1046	1539	615
5d	B_0^2(dd)	6724	6677	6627	6614	4756
	B_0^4(dd)	3841	3840	3746	3820	3010
	B_4^4(dd)	–23864	–23885	–23443	–23760	–22452
	ζ_{5d}	874	930	984	1145	996

a) calculated in this work; b) derived from the experimental data in Ref. [17].

Table 2 lists the experimental and calculated energy levels of Ce^{3+} in YPO_4. The experimental energy levels are taken from Ref. [8]. The biggest difference between the calculated energy levels and the corresponding experimental energy levels is less than 1000 cm^{-1}.

The electric dipole oscillator spectrum for Ce^{3+} is plotted in Fig. 1. The vertical sticks represent the calculated electric dipole oscillator strengths for zero-phonon lines, and the curve is the calculated spectrum

obtained using the method given in subsection 2.3. The dot-dashed curve is the experimental ultraviolet-excited spectrum for monitoring the emission of $5d^1$ to $4f^1$ at 317 nm at room temperature. The excitation spectrum of Ce^{3+} shows five broad bands with maxima at 323, 248, 237, 227 and 203 nm. The band near 150 nm is due to host absorption.

Figure 2 shows the calculated and experimental spectra of Pr^{3+} in YPO_4. The dot-dashed curve is the experimental vacuum ultra violet (VUV)-excited spectrum obtained by monitoring the lowest $4f^15d^1$ to ground state $^3H_5$ emission at 247 nm at room temperature. The bands with maxima at 227, 187, 176 and 160 nm are related to the transitions to the crystal-field component of the 5d electron.

Table 2. Calculated and measured 4f and 5d energy levels of Ce^{3+} doped in YPO4 (units: cm^{-1}).

	D_{2d} (IR)	Experiment[a)]	Calculation[b)]
$4f^1$	Γ_6	0	0
	Γ_7		199
	Γ_6		365
	Γ_6		2166
	Γ_7		2194
	Γ_7		2567
	Γ_6		2619
$5d^1$	Γ_7	30698	29773
	Γ_6	40058	40562
	Γ_6	41929	41746
	Γ_7	43788	44435
	Γ_7	48996	48951

IR is the irreducible representation. a) Experiment energy levels from Ref. [8]; b) DV-Xα calculation.

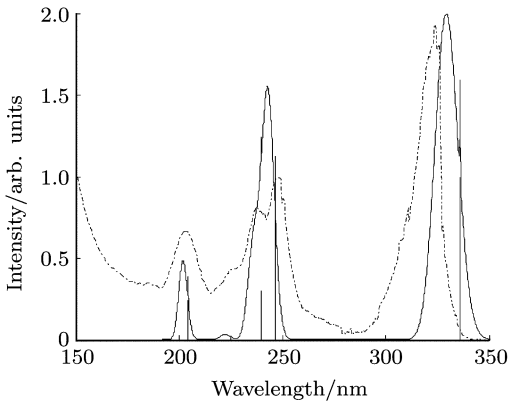


Fig. 1. The spectra of YPO_4: Ce^{3+}. The vertical sticks and solid curve are the calculated electronic dipole oscillator strengths for the zero-phonon lines and the calculated spectrum, respectively. The dot-dashed curve is the excited spectrum measured by monitoring the 5d→4f emission of 335 nm at room temperature.

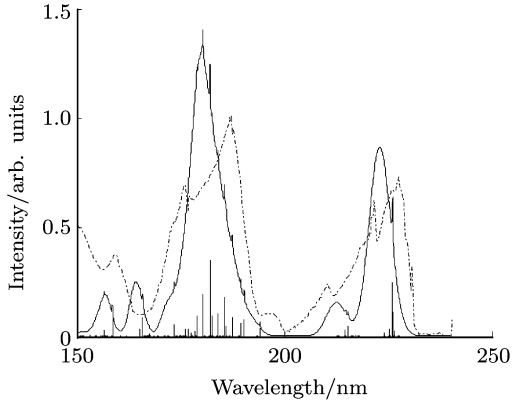


Fig. 2. The spectra of YPO_4: Pr^{3+}. The vertical sticks and solid curve are the calculated electronic dipole oscillator strengths for the zero-phonon lines and the calculated spectrum, respectively. The dot-dashed curve is the excited spectrum measured by monitoring the $4f^15d^1 \rightarrow {}^3H_5$ emission of 247 nm at room temperature.

Figure 3 shows the calculated and experimental spectra of Nd^{3+} in YPO_4. The dot-dashed curve is the observed VUV excited spectrum obtained by monitoring the lowest $4f^25d^1$ to ^4I_J emission at 197 nm at room temperature. The bands with maxima at 186, 160 and 156 nm are related to the transitions to the crystal-field component. The highest crystal field energy level of 5d is calculated to be located at 140 nm, which is absent in the excitation spectrum due to the strong absorption of the host lattice that prevents the excitation light from reaching Nd^{3+} ions inside the crystal.

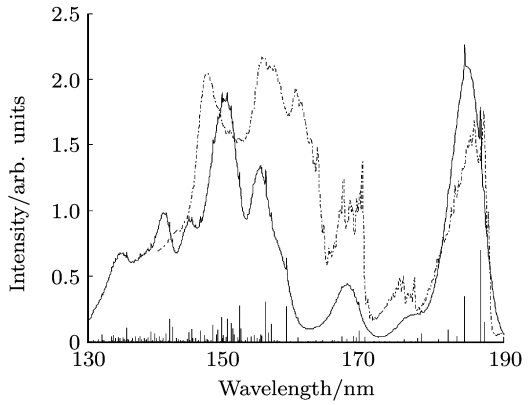


Fig. 3. The spectra of YPO_4: Nd^{3+}. The vertical sticks and solid curve are the calculated electronic dipole oscillator strengths for the zero-phonon lines and the calculated spectrum, respectively. The dot-dashed curve is the excited spectrum measured by monitoring the $4f^25d^1 \rightarrow 4I_J$ emission of 197 nm at room temperature.

Figure 4 shows the calculated and experimental spectra of Eu^{3+} in YPO_4. The dot-dashed curve is the experimental VUV excited spectrum by monitor-

ing $^5D_0$ to $^7F_4$ emission at 700 nm at room temperature. For Eu^{3+} in YPO_4, the charge transfer state is at a lower energy than the $4f^5$5d state. The broad charge transfer excitation band is shown in the range from 160 to 240 mm. The transition to the lowest 5d crystal-field component is observed near 152 nm and split to four peaks due to the direct and exchange Coulomb interactions between the $4f^{N-1}$ core and the 5d electron, which is also shown in the calculated lines. The transitions of the other 5d crystal-field components are calculated to be in the range from 120 to 140 nm in the calculated spectrum, which is again absent in the excitation spectrum due to the strong absorption of the host lattice, which prevents the excitation light from reaching the Nd^{3+} ions inside the crystal.

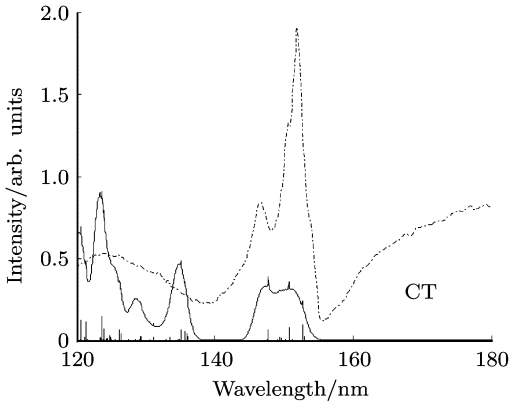


Fig. 4. The spectra of YPO_4: Eu^{3+}. The vertical sticks and solid curve are the calculated electronic dipole oscillator strengths for the zero-phonon lines and the calculated spectrum, respectively. The dot-dashed curve is the excited spectrum measured by monitoring the $^5D_0 \rightarrow {}^7F_4$ emission of 700 nm at room temperature.

4. Conclusions

The method of extracting crystal-field and spin-orbit parameters via the model-space effective Hamiltonian from DV-Xα calculations has been applied separately to Ce^{3+}, Pr^{3+}, Nd^{3+} and Eu^{3+} ions occupying a site of D_{2d} symmetry in a YPO_4 crystal. The calculated 5d energy levels for Ce^{3+} are consistent with the measured results. The energy levels and wave functions for Ce^{3+}, Pr^{3+}, Nd^{3+} and Eu^{3+} ions have also been calculated using the parameters extracted from DV-Xα and other parameters. The observed bands for the $4f^N$–$4f^{N-1}$5d transitions are reasonably consistent with the calculated peaks. The result indicates that the combination of quasi-free ion parameters given in the literature with the crystal-field parameters obtained using the model-space effective Hamiltonian constructed with data from *ab-initio* calculations can be successfully applied to low-symmetry lanthanide systems.

References

[1] Li P L, Yang Z P, Wang Z J and Guo Q L 2008 *Chin. Phys.* B **17** 1907

[2] Zhou T L, Song Z, Song X P, Bian L and Liu Q L 2010 *Chin. Phys.* B **19** 127808

[3] Reid M F, van Pieterson L, Wegh R T and Meijerink A 2000 *Phys. Rev.* B **62** 14744

[4] Duan C K and Tanner P A 2008 *J. Phys.: Condens. Matter* **20** 215228

[5] Duan C K and Tanner P A 2010 *J. Phys. Chem.* A **114** 6055

[6] Zhang Q L, Ning K J, Xiao J, Ding L H, Zhou W L, Liu W P, Yin S T and Jiang H H 2010 *Chin. Phys.* B **19** 087501

[7] Xiao J, Zhang Q L, Zhou W L, Tan X L, Liu W P, Yin S T, Jiang H H, Xia S D and Guo C X 2010 *Acta Phys. Sin.* **59** 7306 (in Chinese)

[8] van Pieterson L, Reid M F, Wegh R T, Soverna S and Meijerink A 2002 *Phys. Rev.* B **65** 045113

[9] Sánchez-Sanz G, Seijo L and Barandiarán Z 2009 *J. Chem. Phys.* **131** 024505

[10] Andriesson J, van der Kolk E and Dorenbos P 2007 *Phys. Rev.* B **76** 075124

[11] Hu L, Reid M F, Duan C K, Xia S and Yin M 2011 *J. Phys.: Condens. Matter* **23** 045501

[12] Reid M F, Duan C K and Zhou H W 2009 *J. Alloys Comp.* **488** 591

[13] Carnall W T, Goodman G L, Rajnak K and Rana R S 1989 *J. Chem. Phys.* **90** 3443

[14] Gschneidner Jr K A, Bunzli J C G and Pecharsky V K 2007 *Handbook on the Physics and Chemistry of Rare Earth* (Amsterdam: North-Holland) pp. 60–98

[15] Rosen A and Ellis D E 1975 *J. Chem. Phys.* **62** 3039

[16] Adachi H, Tsukada M and Satoko C 1978 *J. Phys. Soc. Japan* **45** 875

[17] Williams G M, Becket P C, Conway J G, Edelstem N, Boatner L A and Abraham M M 1989 *Phys. Rev.* B **40** 4132